



Mesoporous phenolic resin and mesoporous carbon for the removal of S-Metolachlor and Bentazon herbicides

Rocío Otero^a, Dolores Esquivel^b, María A. Ulibarri^a, Francisco J. Romero-Salguero^c, Pascal Van Der Voort^{b,*}, José M. Fernández^{a,*}

^a Departamento de Química Inorgánica e Ingeniería Química, Instituto Universitario de Química Fina y Nanoquímica (IUQFN), Campus de Rabanales, Universidad de Córdoba, Campus de Excelencia Internacional Agroalimentario (CeiA3), Córdoba, Spain

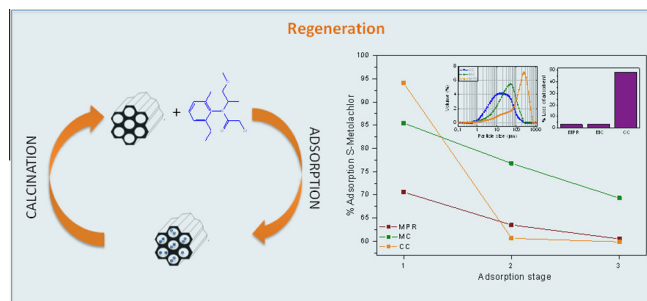
^b Department of Inorganic and Physical Chemistry, Center for Ordered Materials, Organometallics and Catalysis (COMOC), Ghent University, Krijgslaan 281, Building S3, 9000 Ghent, Belgium

^c Departamento de Química Orgánica, Instituto Universitario de Química Fina y Nanoquímica (IUQFN), Campus de Rabanales, Universidad de Córdoba, Campus de Excelencia Internacional Agroalimentario (CeiA3), Córdoba, Spain

HIGHLIGHTS

- Mesoporous carbon is an efficient adsorbent of S-Metolachlor and Bentazon.
- Mesoporous carbon can be reused with a small loss of adsorption capacity.
- Commercial carbon undergoes the highest loss of material during the regeneration.

GRAPHICAL ABSTRACT



ARTICLE INFO

Article history:

Received 8 February 2014

Received in revised form 5 April 2014

Accepted 10 April 2014

Available online 24 April 2014

Keywords:

S-Metolachlor

Bentazon

Mesoporous phenolic resin

Mesoporous carbon

Water treatment

ABSTRACT

Two mesoporous materials, i.e., a mesoporous phenolic resin and a mesoporous carbon, were synthesized following a soft template method to test the removal of two pesticides, Bentazon and S-Metolachlor. The adsorbents were characterized by X-ray diffraction analysis, nitrogen adsorption–desorption isotherms, thermogravimetric analysis, transmission electron microscopy, particle size measurement and XPS spectroscopy. Bentazon and S-Metolachlor adsorption kinetics and isotherm studies were carried out at pH 2 and 4, respectively, on these mesoporous materials as well as on a reference commercial carbon. Freundlich, Langmuir, Dubinin–Raduskevich and Temkin models were applied to describe the adsorption behavior with the Langmuir model showing the best fit. The regeneration of the adsorbents was carried out by calcination under nitrogen atmosphere and the results indicated that the regeneration of the mesoporous carbon was more efficient than that of the mesoporous phenolic resin and the commercial carbon after being reused several times. Another disadvantage of commercial carbon was the great loss of material that it experienced after several adsorption–desorption cycles.

© 2014 Elsevier B.V. All rights reserved.

* Corresponding authors. Tel.: +32 92644442; fax: +32 92644983 (P. Van Der Voort). Tel.: +34 957218648; fax: +34 957580644 (J.M. Fernández).

E-mail addresses: pascal.vandervoort@ugent.be (P. Van Der Voort), um1feroj@uco.es (J.M. Fernández).

1. Introduction

Currently, the pollution caused by pesticides has greatly increased due to their widespread use in agriculture. Pesticides are highly noxious, sometimes non-biodegradable and very mobile

throughout the environment [1]. Therefore, many researchers are studying the removal of these toxic pollutants from aqueous solutions. Photocatalysis [2–4], adsorption [5–7] and electrolysis [8–10] are some processes involved in the removal of these pollutants. The main advantages of adsorption compared to other techniques are its low cost, high removal efficiency and easy operation.

Activated carbons and silica gels have been considered as excellent adsorbents for many years. These materials are not suitable as adsorbents of large molecules because they are mainly microporous [11]. Recently, new mesoporous materials that show promising results for the adsorption of large pollutants have been developed [12–17]. Ordered mesoporous materials possess tunable and uniform pore sizes, large surface areas and large pore volumes.

Among them, the ordered mesoporous polymer resin and mesoporous carbon (MPR and MC) are relatively new materials that combine the high porosity of mesoporous materials with the physicochemical properties of organic polymers and carbons, respectively [18]. MC is an excellent adsorbent and therefore, as carbon is inert, stable, hydrophobic, light and presents a high affinity towards organic pollutants. Ordered mesoporous carbons were firstly synthesized by a hard template method using mesoporous silica [19–21]. However, this synthesis cannot be used for large scale production because it is time-consuming and expensive. Later, a direct synthesis method using phenolic resin as a carbon precursor was developed [22–24].

S-Metolachlor is a selective herbicide used in several crops. It is quite mobile and although it is mainly found in surface water, it can contaminate groundwater. Several authors have investigated the adsorption of this herbicide on different materials, such as activated carbon [25], soil [26], organohydrotalcites [5] or periodic mesoporous organosilicas (PMOs) [6]. Bentazon is a contact post-emergence herbicide widely used in agriculture, which has a great mobility in soil and is moderately persistent in water. That is why previous papers have reported the removal of Bentazon mainly using activated carbon as adsorbent [1,27,28]. The maximum concentration of S-Metolachlor and Bentazon admitted by the World Health Organization (WHO) in drinking water are 0.01 mg/L and 0.03 mg/L, respectively.

Unlike activated carbons, mesoporous phenolic resins and mesoporous carbons have been hardly used as adsorbents of pesticides. Herein we have synthesized two mesoporous materials (MPR and MC) to be tested as regenerable adsorbents for removing S-Metolachlor and Bentazon. MPR has been prepared by the EISA method (evaporation induced self-assembly) [29,30], using resorcinol and formaldehyde in the presence of surfactant F127 (EO₁₀₆–PO₇₀–EO₁₀₆) under acid conditions. MC was synthesized by calcination of MPR. For comparison, a commercially available activated carbon (CC) was also used as adsorbent. The adsorbents were characterized by several structural and surface techniques. Different experiments have been carried out to study the influence of different factors, such as pH and contact time, adsorption/desorption behavior and regeneration of the adsorbents. Finally, adsorption experiments at different temperatures have been undertaken in order to determine thermodynamic parameters.

2. Experimental section

2.1. Chemicals

Pluronic127 (EO₁₀₆PO₇₀EO₁₀₆), resorcinol and commercial activated carbon were purchased from Sigma–Aldrich.

The pesticides used as adsorbates in the experiments, Bentazon (3-(1-methylethyl)-1*H*-2,1,3-benzothiadiazin-4(3*H*)-one 2,2-dioxide) and S-Metolachlor (2-chloro-*N*-(2-ethyl-6-methylphenyl)-*N*-

[(1*S*)-2-methoxy-1-methylethyl]acetamide) were purchased from Sigma Aldrich. Some of their properties are included in Table 1.

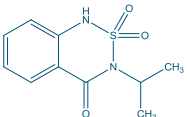
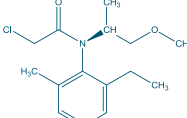
2.2. Synthesis of adsorbents

The synthesis of phenolic resin and mesoporous carbon was carried out using a soft-template method [18]. For that, 9 ml of 3 M HCl were added to a solution of 2.2 g of triblock copolymer Pluronic F127 and 2.2 g of resorcinol in 9 ml of ethanol. After stirring for at least 20 min [31], a formaldehyde solution (2 ml, 36 wt%) was slowly added to it. Then, the mixture was stirred for 20 min. The resultant solution was transferred to a plate to evaporate ethanol. Afterwards, the product was cured in an oven at 60 °C overnight. Finally, the solid was calcined at 380 °C under inert atmosphere to remove the template. The resulting material, a mesoporous phenolic resin, was designed as MPR. Amorphous mesoporous carbon, designed as MC, was obtained by calcination of MPR in a tubular furnace under inert atmosphere at 800 °C.

2.3. Characterization

Mesoporous phenolic resin and mesoporous carbon were characterized by different techniques. Powder X-ray diffraction (XRD) patterns were recorded with a Thermo Scientific ARL X'TRA Powder X-ray Diffraction System (radiation Cu K α generated by 45 kV and 44 mA, with slits of 2, 4, 1.5 and 0.2 for the divergence, scatter, receiving scatter and receiving slit, respectively, at 0.25° 2 θ min⁻¹). Nitrogen adsorption–desorption isotherms were obtained on a Bel-sorp-mini II gas analyser. Prior to the measurements, the samples were degassed at 120 °C for 24 h to remove adsorbed water. Thermogravimetric curves were recorded on a Setaram Setsys Evolution 16/18 apparatus under nitrogen at a heating rate of 5 °C/min. Microstructural characterization of the materials was carried out using JEOL 1400 TEM and JEOL 2010 TEM equipments. Particle sizes were measured in a Mastersizer S analyser (Malvern Instruments) using ethanol as dispersant. The samples were sonicated for 10 min before the analysis. XPS spectra were recorded with a SPECS Phoibos HAS 3500 150 MCD. The residual pressure in the analysis chamber was 5 · 10⁻⁹ Pa. The X-ray source was generated by a Mg anode ($h\nu = 1253.6$ eV) powered at 12 kV and with an emission current of 25 mA. The powdered sample was pressed and introduced into the spectrometer without previous thermal treatment. They were outgassed overnight and analyzed at room temperature. Accurate binding energies (BE) have been determined with respect to the position of the C 1s peak at 284.9 eV. The surface atomic concentration ratios were calculated using sensitivity factors from the Casa XPS element library. The potential zeta (ζ) has been determined with a Zetasizer Nano ZS (Malvern Instruments), with a laser of 632.8 nm, coupled to a MPT-2 autotitrator.

Table 1
Properties of pesticides Bentazon and S-Metolachlor.

Pesticide	Structure	MW (g/mol)	S (mg/L)	pK _a
Bentazon		240.3	570	3.3
S-Metolachlor		283.79	480	–

2.4. Adsorption experiments

All adsorption experiments were carried out in duplicate by using the batch equilibration technique at 25 ± 1 °C. Adsorption of Bentazon (25–250 mg/L) and S-Metolachlor (125–400 mg/L) were conducted by mixing 20 mg of adsorbent with 30 mL of pesticide solution and stirring continuously the mixture for 24 h. The suspension was centrifuged and the concentration of Bentazon and S-Metolachlor were determined by UV–Vis spectroscopy at 232 nm and 265 nm, respectively, on a Perkin Elmer Lambda 11 UV–Vis spectrophotometer.

The adsorption kinetics were investigated by three models, the Lagergren pseudo-first-order model [32], the pseudo-second-order-model [33] and intraparticle diffusion model [34].

$$\log(C_s - C_{st}) = \log C_s - \frac{k_1}{2.303} \cdot t \quad (1)$$

$$\frac{t}{C_{st}} = \frac{1}{k_2 \cdot C_s^2} + \frac{1}{C_s} \cdot t \quad (2)$$

$$C_{st} = k_p \cdot t^{1/2} + C \quad (3)$$

where k_1 is the pseudo first order rate constant for the adsorption process (h^{-1}), C_s and C_{st} (mg g^{-1}) are the amounts of adsorbed pesticide at equilibrium and at time t (h), respectively, k_2 is the rate constant of pseudo-second-order adsorption ($\text{g mg}^{-1} \text{h}^{-1}$) and k_p ($\text{mg g}^{-1} \text{h}^{-1/2}$) is the intraparticle diffusion rate constant.

The equilibrium experimental adsorption data were fitted to Freundlich [35], Langmuir [36], Temkin [37] and Dubinin–Raduskevich [38] models and the estimated parameters calculated from the fitting results are reported in Table 4.

The Freundlich model assumes that the adsorption occurs on a heterogeneous surface. The logarithmic equilibrium expression of this model is:

$$\log C_s = \log K_f + n_f \log C_e \quad (4)$$

where K_f ($\text{mg}^{1-n_f} \text{L}^{n_f} \text{g}^{-1}$) and n_f are the Freundlich constants indicative of adsorption capacity and adsorption intensity, respectively.

The Langmuir model describes the adsorbate–adsorbent interactions and is based on the assumption that the adsorption energy is constant and independent of the surface coverage. Its expression is:

$$\frac{1}{C_s} = \frac{1}{C_m} + \frac{1}{C_m \cdot L \cdot C_e} \quad (5)$$

where C_m (mg g^{-1}) is the monolayer capacity of the adsorbent and L (L mg^{-1}) is the Langmuir adsorption constant.

Temkin model describes the behavior of adsorption on heterogeneous surfaces. This model is based on the heat of adsorption (due to the interactions between adsorbate and adsorbent). The Temkin isotherm has generally been applied in the following form:

$$C_s = B_T \ln K_T + B_T \ln C_e \quad (6)$$

where K_T and B_T are constants related to adsorption capacity and intensity of adsorption, respectively.

The isotherm of desorption was measured at each equilibrium point in the adsorption curve by replacing 7.5 mL of supernatant with an identical volume of distilled water. After shaking for 24 h, the amount of herbicide desorbed was calculated as indicated above. This procedure is described in detail elsewhere [5].

The isotherms of adsorption were studied at three constant temperatures: 10, 20 and 30 °C for Bentazon and S-Metolachlor. To test the reversibility, the adsorbents were subjected to three adsorption–desorption cycles. The desorption from mesoporous phenolic resin was carried out by calcination under nitrogen at

380 °C for 4 h; mesoporous carbon and commercial carbon were treated under nitrogen at 400 °C for 4 h.

3. Results and discussion

3.1. Characterization of the materials

The XRD-patterns of the mesoporous phenolic resin (MPR) and the mesoporous carbon (MC) exhibited a low angle (100) peak with d -spacing of 11.6 nm and 10.3 nm, respectively (Fig. 1). Additional peaks at higher incidence angles were ill-defined [39]. Their mesoporous structures were confirmed by TEM images (Fig. 2). The pore channels with hexagonal arrangement suggest an ordered mesostructure. The size of these channels was around 10 nm (see insets in Fig. 2b and c). However, no ordering was observed in the commercial carbon (Fig. 2a). Moreover, the N_2 adsorption–desorption isotherms for MPR and MC were essentially of type IV (Fig. 3) with a sharp capillary condensation step at $P/P_0 = 0.45$ – 0.57 , which is typical of mesoporous materials as defined by IUPAC [40]. Nevertheless, the commercial carbon exhibited a type I isotherm, which corresponds to a microporous material. MC had a slightly higher surface area than MPR. This is probably due the formation of micropores as a consequence of the decomposition of the phenolic framework of MPR to obtain the mesoporous carbon as shown in the TGA curve between 500 and 750 °C (Fig. 4). The pore size for MPR and MC was around 9 nm (inset in Fig. 3), in agreement with TEM. The main physicochemical properties of the two mesoporous adsorbents (MPR and MC) along with those of the commercial carbon are listed in Table 2.

The particle size distribution curves of MPR and MC are shown in Fig. 5. MPR displayed a considerably large particle size with the main peak centered at about 250 μm . Interestingly, the distribution of particle size for MC was wider and clearly shifted to lower values (ca. 50 μm). This revealed the significant reduction of the particle size upon carbonization of the MPR to MC. The curve for CC was very broad and centered between 10 and 30 μm , showing a significantly lower particle size than MPR and MC.

Surface analyses obtained by XPS for the three adsorbents are depicted in Table 2. MPR possessed a significant amount of oxygen, as expected from the composition of the polymer. The fraction of oxygen decreased as a result of the transformation of MPR into MC, which involves the deoxygenation of the phenolic groups, among other reactions. CC also presented a considerably amount of oxygen which was much higher than that of MC. The C 1s and O 1s XP spectra are represented in Fig. 6. The large FWHM (full

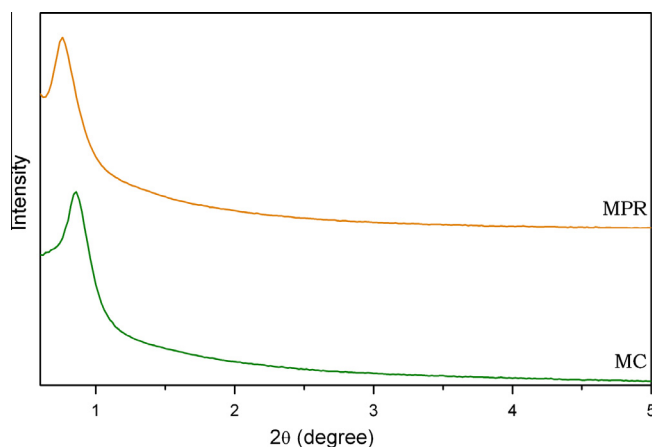


Fig. 1. Powder X-ray diffraction patterns of mesoporous phenolic resin (MPR) and mesoporous carbon (MC).

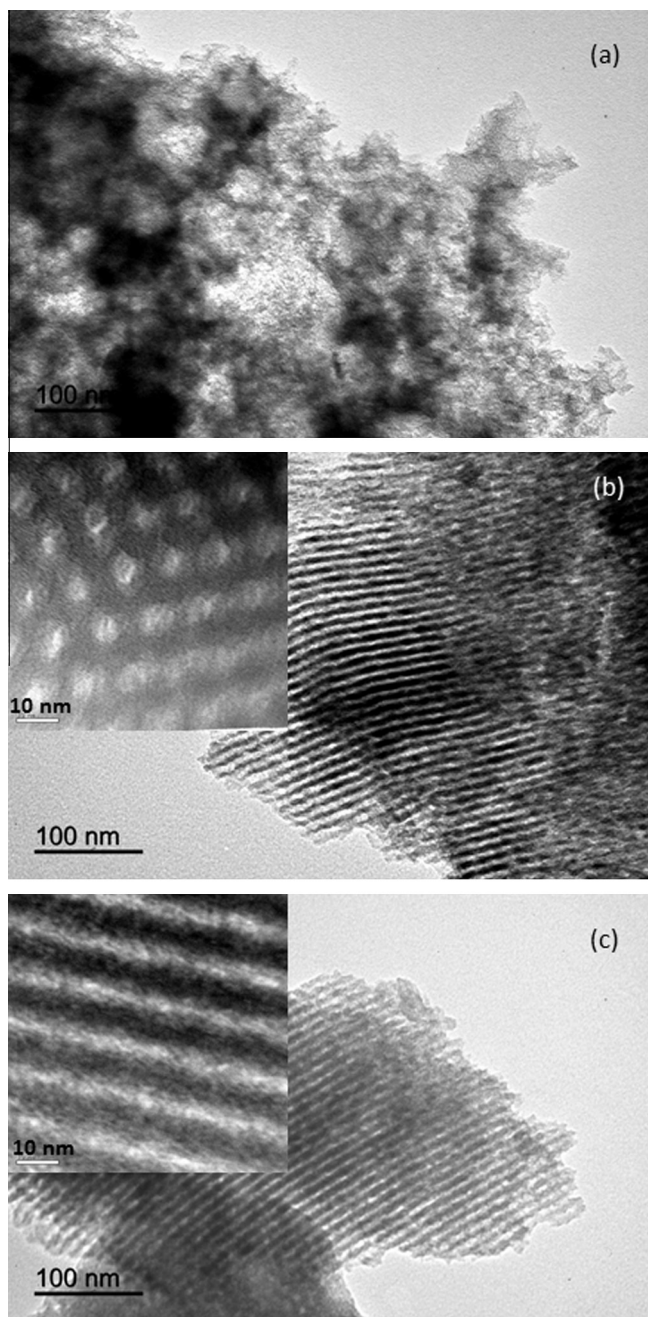


Fig. 2. TEM images for commercial carbon (CC) (a), mesoporous phenolic resin (MPR) (b), including a TEM image of high resolution (inset), and mesoporous carbon (MC) (c), including a TEM image of high resolution (inset).

width at half-maximum) values of the peaks (1.4–2.7 eV for C 1s and 2.9–3.6 eV for O 1s) suggested the existence of different carbon and oxygen species. Obviously, MPR exhibited various types of carbon atoms, namely C–C, C=C and C–O. MC displayed the narrowest C 1s peak due to the major presence of aromatic carbon atoms in its framework whereas CC even showed additional small contributions at high binding energies indicative of the existence of C=O species. Similarly, the O 1s spectra confirmed the contribution of a higher variety of species in CC than in MPR and MR.

3.2. Adsorption kinetics of Bentazon and S-Metolachlor

The adsorption of Bentazon and S-Metolachlor on the mesoporous materials and the commercial carbon was studied at different

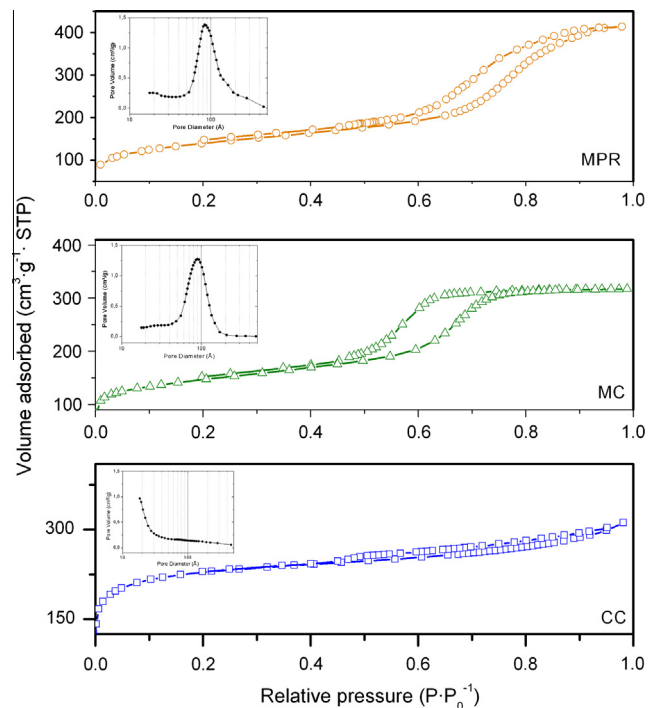


Fig. 3. Nitrogen adsorption–desorption isotherms and the corresponding pore size distributions (insets) for mesoporous phenolic resin (MPR), mesoporous carbon (MC) and commercial carbon (CC).

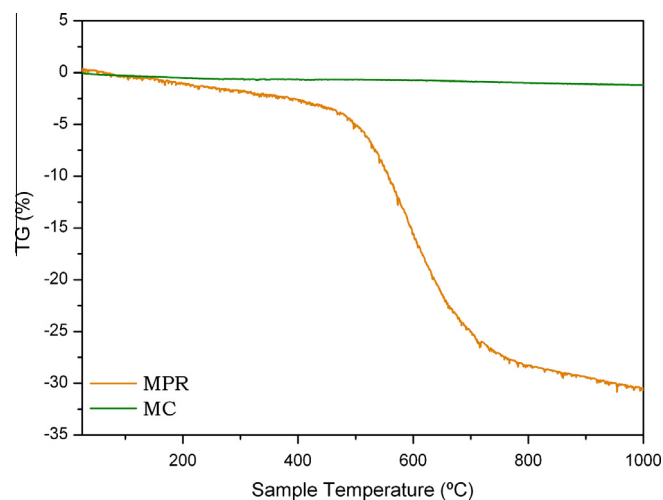


Fig. 4. Thermogravimetric curves for mesoporous phenolic resin (MPR) and mesoporous carbon (MC).

Table 2

Physicochemical properties of commercial carbon, mesoporous phenolic resin and mesoporous carbon.

Sample	S_{BET} ($\text{m}^2 \text{g}^{-1}$)	$S_{\text{micropores}}$ ($\text{m}^2 \text{g}^{-1}$)	V_p^a ($\text{cm}^3 \text{g}^{-1}$)	d_{100} (Å)	C^b (at.%)	O^b (at.%)
CC	688	406	0.41	–	85.93	14.07
MPR	503	160	0.63	116	82.92	14.08
MC	526	294	0.49	103	95.10	4.90

^a Single point total adsorption.

^b C and O determined by XPS.

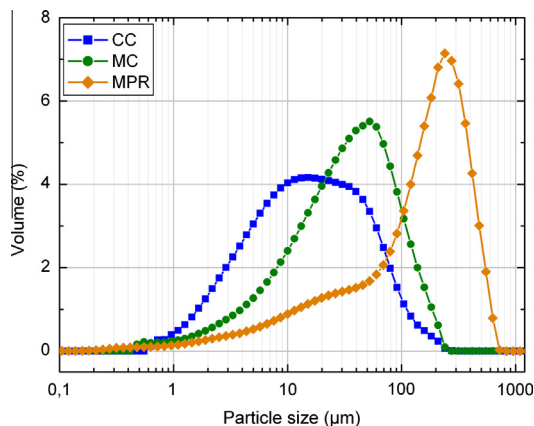


Fig. 5. Particle size distribution curves for mesoporous phenolic resin (MPR), mesoporous carbon (MC) and commercial carbon (CC).

pH values using 30 mL of either 50 mg/L Bentazon or 100 mg/L S-Metolachlor and 20 mg of adsorbent (Fig. 7). An increase in the pH caused a decrease in the adsorption of Bentazon probably due to the enhancement of the electrostatic repulsion between the ionized pesticide and the adsorbent surface [1]. The point of zero

charge (pzc) was determined for the three materials and revealed some differences among them (see Supporting information, Fig. S11). The pzc value indicates the pH required to give zero net surface charge. The pHs were 5.3, 3.2 and 2.7 for commercial carbon, mesoporous carbon and phenolic resin, respectively. When the pH is higher than the pzc, the surface is negatively charged. As pH is increased, the surface is more negatively charged. On the other hand, Bentazon is a weak acid with pK_a of 3.3; and at pH above the pK_a , it exists predominantly in anionic form. As pH is increased, the extent of dissociation of Bentazon molecules is increased and so it becomes more negatively charged. As a result, the equilibrium adsorption of Bentazon decreased with an increase in the pH of the initial solution. This could be attributed to the increased electrostatic repulsion between Bentazon ions and the surface of the three materials [1]. Similar observations were made for the adsorption of Bentazon onto AC cloth [41].

Given the aromatic structure of Bentazon, dispersion forces should be expected between the π cloud of the adsorbents and the aromatic ring of the adsorbate. Also, some specific localized interactions might arise from the polar groups (i.e., sulfoxide and carbonyl-type) [28]. The decrease in the amount adsorbed at higher pH (anionic form predominant in solution) suggests a weaker interaction of the surfaces with deprotonated (anionic) Bentazon than with its neutral form, and consequently that the

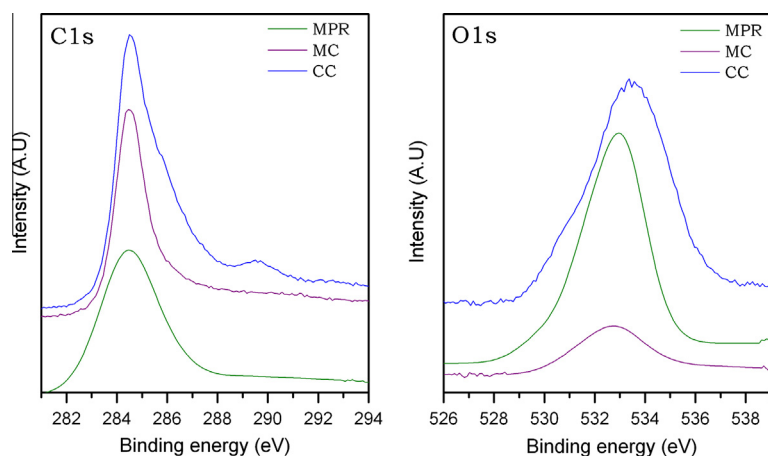


Fig. 6. XPS analysis for mesoporous phenolic resin (MPR), mesoporous carbon (MC) and commercial carbon (CC).

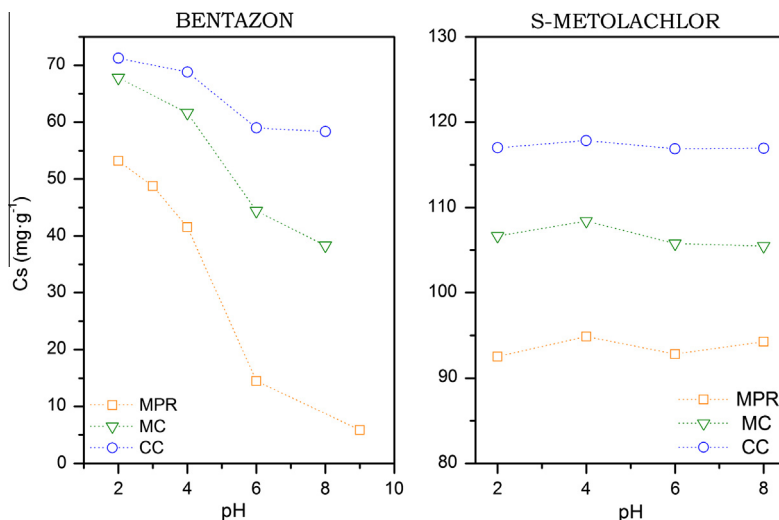


Fig. 7. Influence of pH on the adsorption of S-Metolachlor and Bentazon on mesoporous phenolic resin (MPR), mesoporous carbon (MC) and commercial carbon (CC).

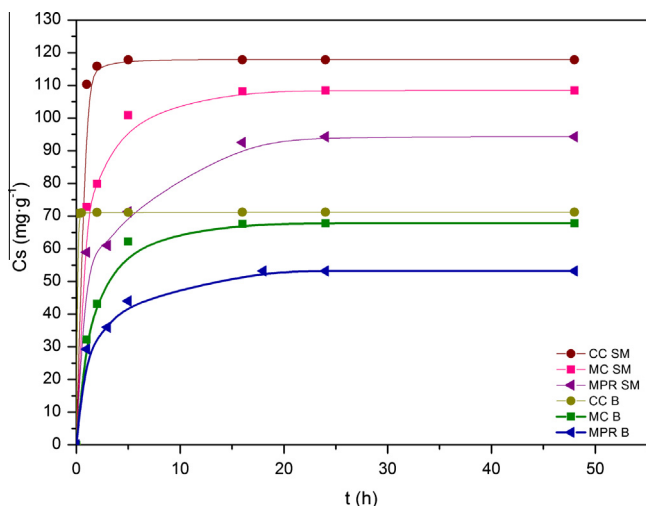


Fig. 8. Adsorption kinetics of S-Metolachlor and Bentazon on mesoporous phenolic resin (MPR), mesoporous carbon (MC) and commercial carbon (CC).

adsorption is dominated by dispersive interactions between the pesticide and the adsorbent surface. Similar results on the pH-dependence of Bentazon adsorption have been reported by other authors [42,43]. In addition, the relative drop in the adsorption was higher when the pH of the point of zero charge was lower (see Figs. 7 and S11). Thus, the phenolic resin was the most affected by changes in the pH.

However, the adsorption of S-Metolachlor on both mesoporous materials, MPR and MC, and the commercial carbon, CC, was not affected by the pH. This could be associated to the non-ionizable nature of S-Metolachlor in the pH range under study. Indeed, the adsorption of S-Metolachlor would occur through π - π interactions between the aromatic ring of the pesticide and π -electrons of the adsorbent structure [41].

The effect of the contact time at the pH of maximum adsorption is depicted in Fig. 8. The adsorption of Bentazon and S-Metolachlor on commercial carbon was fast, reaching the equilibrium in 2 h, while their adsorption on the mesoporous materials was slower (ca. 16 h). These differences in the adsorption kinetics might be explained by the higher specific surface area (Table 2) and smaller particle size (Fig. 5) of CC with respect to both mesoporous materials.

The fitting parameters for the adsorption kinetic of Bentazon and S-Metolachlor on MPR, MC and CC are listed in Table 3. The correlation coefficients R^2 for the pseudo-second-order kinetics (0.999) were best fitted than for a pseudo-first-order kinetics model (0.561–0.995). Similar results were reported by Salman et al. using an activated carbon as adsorbent for two pesticides, Bentazon and Carbofuran [1].

Following the Morris–Weber equation for intraparticle diffusion (Eq. (3)), the plots of C_s versus $t^{1/2}$ consist of straight lines for the

pesticide adsorption on the three adsorbents. The extrapolation of these lines does not pass through the origin, suggesting that intraparticle diffusion cannot be the rate-determining step and other factors may have operated simultaneously to govern the adsorption process [44,45].

Further information about the adsorption mechanism can be obtained analyzing the adsorption isotherm for the systems under study. The isotherms for the adsorption of Bentazon and S-Metolachlor on mesoporous phenolic resin and mesoporous carbon (Fig. 9) were compared with that of commercial carbon (Fig. 10). According to Giles classification [46], the isotherms for Bentazon adsorption on MPR, MC and CC corresponded to a L2 type. Also, S-Metolachlor on CC exhibited a L2 type isotherm. However, the adsorption of S-Metolachlor on MPR and MC gave a L4 type isotherm. In the case of Bentazon, the plateau was reached at C_s value of 130.74 mg g⁻¹, 166.72 mg g⁻¹ and 218.04 mg g⁻¹ for MPR, MC and CC, respectively. By contrast, the second plateau for S-Metolachlor on MPR and MC was not reached, indicating that the maximum adsorption capacity of the adsorbent was not achieved under these conditions. Similar behavior was observed in the adsorption of this pesticide on phenylene-bridged and ethylene-bridged periodic mesoporous organosilicas [6]. The adsorption isotherm of S-Metolachlor on CC exhibited an ill-defined plateau with a value of $C_s = 340.17$ mg g⁻¹.

The fitted parameters of adsorption were calculated from the linear regressions of Eqs. (4)–(6). According to the regression coefficient values, the Langmuir model showed a much better fit than the Freundlich and Temkin models (Table 4).

These models do not give any idea about the mechanism of adsorption. To understand the adsorption type, experimental data were fitted to the Dubinin–Radushkevich (D–R) model:

$$\ln C_s = \ln q_m - K\varepsilon^2 \quad (7)$$

where q_m is the theoretical adsorption capacity of the adsorbent (mg g⁻¹), K (mg² kJ⁻²) is the constant related to adsorption energy and $\varepsilon = RT \ln(1 + 1/C_e)$ is the Polanyi potential.

The adsorption energy (E) can be calculated using the D–R equation and the following relationship has been used.

$$E = (2K)^{-0.5} \quad (8)$$

The adsorption is physical in nature when E is between 0 and 8 kJ mol⁻¹; if it is $8 < E < 16$ kJ mol⁻¹ the adsorption is due to exchange of ions; and if the value of E is between $20 < E < 40$ kJ mol⁻¹, a chemisorption occurs. In the case of S-Metolachlor, the values found in the present study for the three adsorbents were around 8 kJ mol⁻¹ whereas in the case of Bentazon were between 11 and 13 kJ mol⁻¹. Consequently, the adsorption of Bentazon could be explained by exchange of ions. In addition, E values for S-Metolachlor were in the limit between physical adsorption and exchange of ions and so it was not possible to explain precisely the nature of the adsorption.

The desorption curves [5] above the adsorption curves evidenced the difficulty to remove S-Metolachlor and Bentazon from

Table 3

Kinetic parameters for the adsorption of Bentazon and S-Metolachlor onto mesoporous phenolic resin and mesoporous carbon compared with commercial carbon.

Pesticide	Adsorbent	$C_{s, \text{exp}}$	Pseudo first order model			Pseudo second order model			Intraparticle diffusion		
			K_1 (h ⁻¹)	C_{s_1} (mg g ⁻¹)	R^2	K_2 (g mg ⁻¹ h ⁻¹)	C_{s_2} (mg g ⁻¹)	R^2	K_p (mg g ⁻¹ h ^{-1/2})	C (mg g ⁻¹)	R^2
Bentazon	MPR	53.20	0.39	48.97	0.992	0.018	54.64	0.999	4.05	30.62	0.780
	MC	67.82	0.34	43.71	0.991	0.017	69.44	0.999	5.43	38.29	0.652
	CC	71.23	0.23	0.287	0.561	4.9	71.43	0.999	0.06	70.95	0.617
S-Metolachlor	MPR	94.28	0.21	55.40	0.983	$8.4 \cdot 10^{-3}$	97.08	0.999	6.91	54.77	0.829
	MC	108.4	0.32	47.28	0.995	0.019	109.89	0.999	5.82	76.56	0.691
	CC	117.9	1.22	18.28	0.941	0.24	117.65	0.999	0.85	113.36	0.413

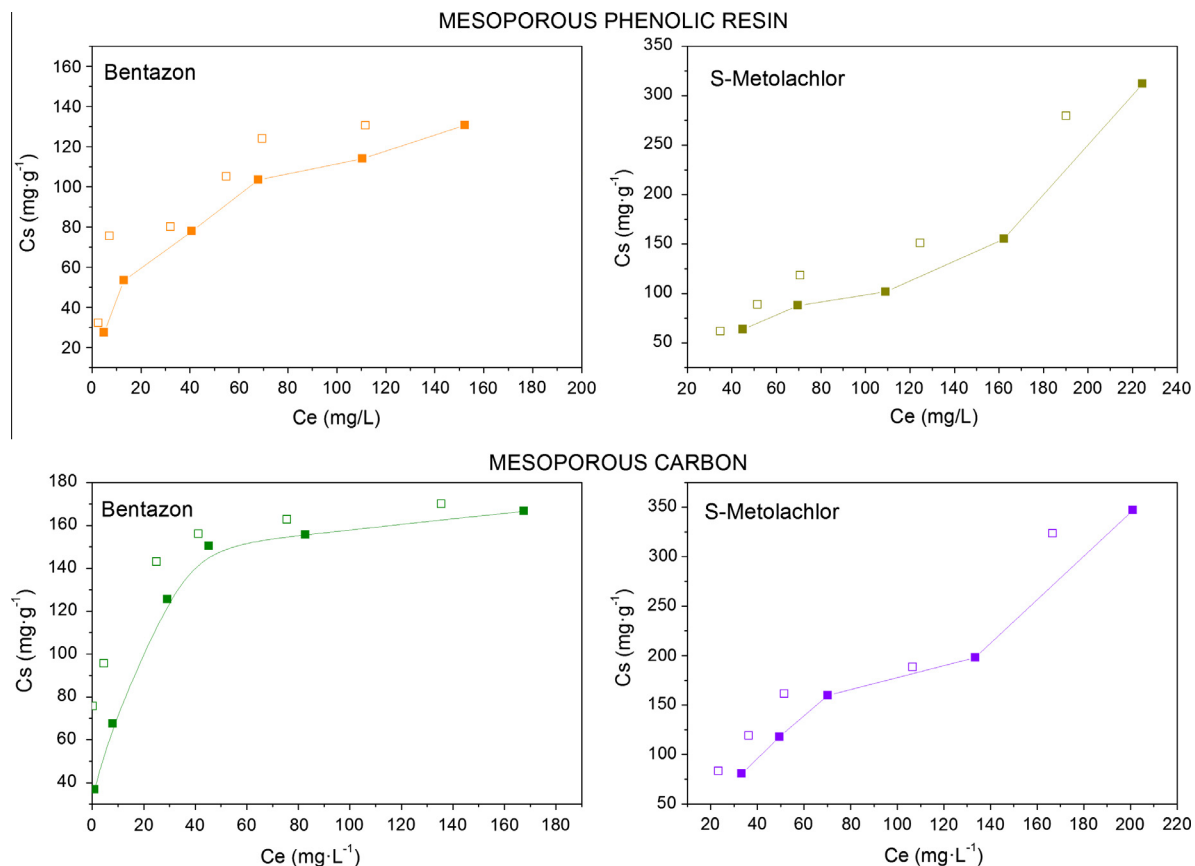


Fig. 9. Adsorption and desorption isotherms of S-Metolachlor and Bentazon on mesoporous phenolic resin (MPR) and mesoporous carbon (MC).

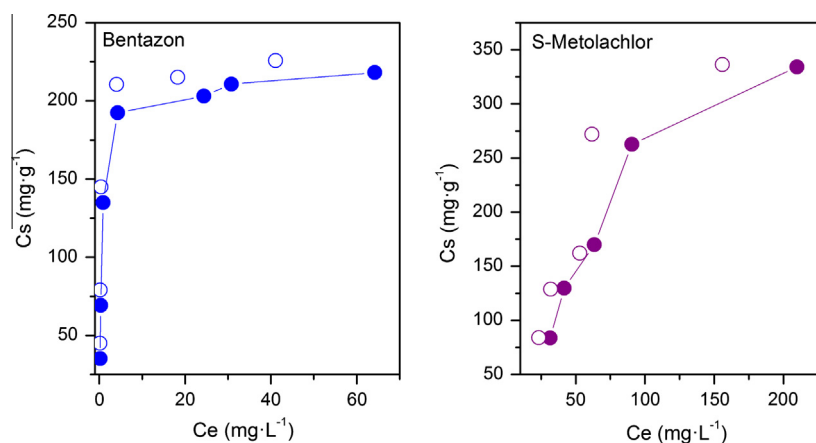


Fig. 10. Adsorption and desorption isotherms of S-Metolachlor and Bentazon on commercial carbon (CC).

Table 4
Freundlich, Langmuir, Dubinin–Ruduskevich and Temkin model parameters for S-Metolachlor and Bentazon adsorption onto mesoporous phenolic resin and mesoporous carbon compared with commercial carbon.

Pesticide	Adsorbent	Freundlich			Langmuir			Dubinin–Ruduskevich			Temkin		
		K_f	n_f	R^2	C_m	L	R^2	q_m	K	R^2	B_T	K_T	R^2
Bentazon	MPR	15.19–13.31	0.44 ± 0.03	0.980	129.20	0.05	0.994	$2.1 \cdot 10^{-3}$	$3.9 \cdot 10^{-3}$	0.986	28.39	0.45	0.984
	MC	42.56–33.96	0.32 ± 0.03	0.964	174.82	0.11	0.998	$1.8 \cdot 10^{-3}$	$2.6 \cdot 10^{-3}$	0.968	27.56	3.09	0.947
	CC	105.86–76.35	0.26 ± 0.06	0.774	219.30	1.04	0.998	$2.6 \cdot 10^{-3}$	$2.0 \cdot 10^{-3}$	0.815	30.17	39.84	0.893
S-Metolachlor	MPR	4.12–0.81	0.90 ± 0.17	0.900	467.28	$3.3 \cdot 10^{-3}$	0.922	0.015	$9.2 \cdot 10^{-3}$	0.884	133.97	0.03	0.748
	MC	9.34–4.33	0.74 ± 0.08	0.921	666.67	$4.2 \cdot 10^{-3}$	0.989	0.012	$7.4 \cdot 10^{-3}$	0.958	133.04	0.05	0.887
	CC	13.83–4.87	0.72 ± 0.12	0.922	1434.7	$2.1 \cdot 10^{-3}$	0.978	0.014	$7.3 \cdot 10^{-3}$	0.937	138.02	0.06	0.960

Table 5

Thermodynamic parameters for S-Metolachlor and Bentazon adsorption onto mesoporous phenolic resin and mesoporous carbon compared with commercial carbon.

Pesticide	Adsorbent	T (°C)	K	ΔS (kJ mol ⁻¹ K ⁻¹)	ΔH (kJ mol ⁻¹)	ΔG (kJ mol ⁻¹)
S-Metolachlor	MPR	10	979	-0.018	-21.16	-16.20
		20	623			-15.67
		30	542			-15.86
	MC	10	11494	0.056	-6.10	-22.00
		20	10042			-22.44
		30	9728			-23.13
Bentazon	MPR	10	82782	0.054	-11.42	-26.64
		20	69192			-27.15
		30	60241			-27.72
	MC	10	36003	0.31	62.87	-24.68
		20	131520			-28.71
		30	208029			-30.85

the adsorbents. The presence of hysteresis (Figs. 9 and 10) indicates the irreversibility of the process in all cases.

3.3. The effect of temperature

In order to determine the thermodynamic parameters of the adsorption of Bentazon and S-Metolachlor on the three adsorbents, the effect of the temperature was studied. When the temperature was increased from 10 to 30 °C the amount of adsorbed Bentazon slightly increased, unlike S-Metolachlor whose adsorption behavior was similar in the whole temperature range.

The change in standard free energy (ΔG°), enthalpy (ΔH°), and entropy (ΔS°) of adsorption was calculated using the following equations (Eqs. (9) and (10)) [47,48]:

$$\Delta G^\circ = \Delta H^\circ - T\Delta S^\circ \quad (9)$$

$$\ln K = \Delta S^\circ / R - \Delta H^\circ / RT \quad (10)$$

where K is the equilibrium constant, R the molar gas constant and T the absolute temperature. The values of ΔH° and ΔS° were calculated from the slope and intercept of Van't Hoff plots ($\ln K_C$ versus $1/T$) and are summarized in Table 5. The values of K have been obtained from the values of K_L from the Langmuir equation because our isotherms were well fitted to this equation. K has been recalculated to become dimensionless by multiplying it by 10^6 [49]. ΔG° values were calculated from Eq. (9). The negative ΔG° values indicate that the process is thermodynamically feasible and spontaneous. In the case of Bentazon, the ΔG° values were slighter higher as the temperature increased indicating that the process was chemically controlled. By contrast, the behavior of S-Metolachlor showed two different tendencies (physical and chemical).

3.4. Regeneration of the adsorbents

To test their reusability, the adsorbents were regenerated by calcination under nitrogen atmosphere at 380 °C for mesoporous phenolic resin and 400 °C for mesoporous carbon and commercial carbon. The adsorbents were subjected to three adsorption-desorption cycles (Fig. 11). The regeneration efficiencies of the mesoporous materials were compared with the commercial carbon. In the third cycle, the adsorption capacity for S-Metolachlor on MPR, MC and CC were 60.5%; 69.29% and 59.85%, respectively, while for Bentazon were 77.33% for MPR; 90.22% for MC and 88.82% for CC. For both pesticides, the regeneration was better in mesoporous carbon than in mesoporous phenolic resin and commercial carbon. The differences between both mesoporous materials can be associated to the presence of more defects in the mesostructure of the phenolic resin than in that of the mesoporous carbon after their regeneration (see Fig. S12 in Supporting

information). In relation to CC, the lower decrease in the adsorption capacity for MC could be ascribed to its mesoporous character and its lower fraction of micropores [50,51]. Similar behavior was described by Suchithra et al. [52], who studied the regeneration of hybrid mesoporous material compared with commercial carbon for the removal of dyes and other organic compounds.

A great disadvantage of the commercial carbon compared to the mesoporous materials in relation to their reusability was its significant loss of material after several adsorption-desorption cycles. After three cycles, the losses of the commercial adsorbent were 48.2% and 47.1% for the adsorption of S-Metolachlor and Bentazon, respectively, while it was less than 5% for the mesoporous materials (Fig. 11). After each adsorption cycle the material was recovered with a filter of 0.45 μm of pore size, which should retain all particles according to the particle size distribution depicted in Fig. 5. However, these results suggest that the commercial carbon undergoes a shear degradation that decreases the particle size, thus allowing the resulting smallest particles to pass through the filter. The loss of this material involves serious concerns for its practical application because it reduces drastically its durability, unlike both mesoporous materials, which proven to be more resistant to friction.

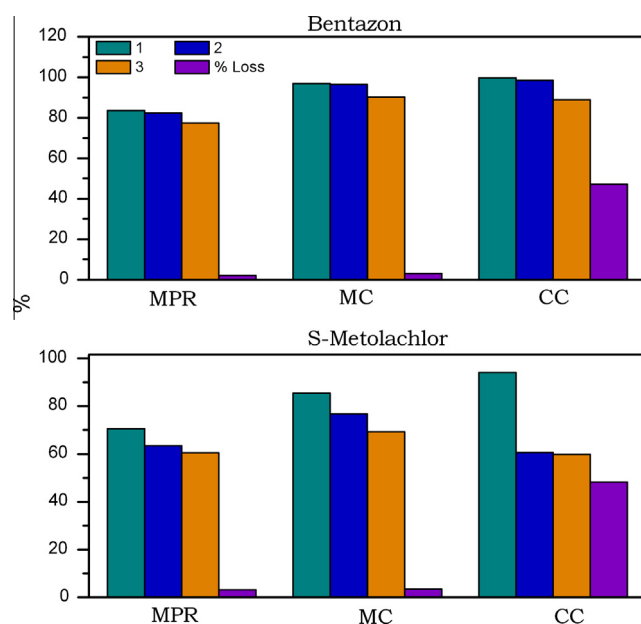


Fig. 11. Adsorption-desorption cycles for S-Metolachlor and Bentazon. Adsorption after first (1), second (2) and third (3) cycle. Weight lost after three adsorption-desorption cycles (% loss).

4. Conclusions

Mesoporous phenolic resin and mesoporous carbon exhibited good properties to be used as adsorbents in virtue of their high surface area and narrow mesopore distribution. The N₂ adsorption-desorption isotherms for MPR and MC were essentially of type IV. The pore size of these materials was around 9–10 nm according to the N₂ adsorption and TEM results. We have examined a potentially practical use of these materials for the adsorption of S-Metolachlor and Bentazon. The adsorption of these pollutants varied with the pH. The adsorption of Bentazon decreased when the pH increased, probably due to the increase of the electrostatic repulsion between the pesticide ion and the adsorbent surface. By contrast, the adsorption of S-Metolachlor was not affected by the pH.

The adsorption kinetics fitted better to a pseudo-second-order kinetics model. Intraparticle diffusion was present in the adsorption process together with other factors. The isotherms for Bentazon on MPR, MC and CC and for S-Metolachlor on CC were of L2 type while the adsorption of S-Metolachlor on MPR and MC exhibited a L4 type isotherm. In the case of Bentazon, a plateau was reached for the three adsorbents. By contrast, the second plateau for S-Metolachlor on MPR and MC was not reached, indicating that the maximum capacity of these adsorbents was not achieved under these conditions. In all cases the Langmuir model showed a much better fit. The adsorption of Bentazon could be explained as exchange of ions according to the Dubinin–Radushkevich model. The presence of hysteresis in the desorption curves indicated irreversibility of the process in all cases.

The regeneration efficiency was better in mesoporous carbon than in mesoporous phenolic resin and commercial carbon for both pesticides. Another disadvantage of the commercial carbon compared to the mesoporous materials for their regeneration was the great loss of material after successive adsorption-desorption cycles.

Acknowledgements

The authors wish to acknowledge funding of this research by Ministerio de Ciencia e Innovación (Project MAT2010-18778) and Junta de Andalucía (Project P06-FQM-01741). D.E. is a postdoctoral researcher of the FWO-Vlaanderen (Fund Scientific Research – Flanders), Grant Number 3E10813W. R. Otero acknowledges Ministry of Education and Science for a research and teaching fellowship.

Appendix A. Supplementary material

Supplementary data associated with this article can be found, in the online version, at <http://dx.doi.org/10.1016/j.cej.2014.04.038>.

References

- [1] J.M. Salman, V.O. Njoku, B.H. Hameed, Bentazon and carbofuran adsorption onto date seed activated carbon: kinetics and equilibrium, *Chem. Eng. J.* 173 (2011) 361–368.
- [2] C.D. Stan, I. Cretescu, C. Pastravanu, I. Poullos, M. Dragan, Treatment of pesticides in wastewater by heterogeneous and homogeneous photocatalysis, *Int. J. Photoenergy* (2012), <http://dx.doi.org/10.1155/2012/194823>.
- [3] S. Rafqah, P. Wong-Wah-Chung, A. Aamili, M. Sarakha, Degradation of metsulfuron methyl by heterogeneous photocatalysis on TiO₂ in aqueous suspensions: kinetic and analytical studies, *J. Mol. Catal. A: Chem.* 237 (2005) 50–59.
- [4] X. Zhu, C. Yuan, Y. Bao, J. Yang, Y. Wu, Photocatalytic degradation of pesticide pyridaben on TiO₂ particles, *J. Mol. Catal. A: Chem.* 229 (2005) 95–105.
- [5] R. Otero, J.M. Fernandez, M.A. Ulibarri, R. Celis, F. Bruna, Adsorption of non-ionic pesticide S-Metolachlor on layered double hydroxides intercalated with dodecylsulfate and tetradecanedioate anions, *Appl. Clay Sci.* 65–66 (2012) 72–79.
- [6] R. Otero, D. Esquivel, M.A. Ulibarri, C. Jiménez-Sanchidrián, F.J. Romero-Salguero, J.M. Fernández, Adsorption of the herbicide S-Metolachlor on periodic mesoporous organosilicas, *Chem. Eng. J.* 228 (2013) 205–213.
- [7] O.A. Ioannidou, A.A. Zabaniotou, G.G. Stavropoulos, M.A. Islam, T.A. Albanis, Preparation of activated carbons from agricultural residues for pesticide adsorption, *Chemosphere* 80 (2010) 1328–1336.
- [8] R.-H. Chen, L.-Y. Chai, Y.-Y. Wang, H. Liu, Y.-D. Shu, J. Zhao, Degradation of organic wastewater containing Cu–EDTA by Fe–C micro-electrolysis, *Trans. Nonferr. Met. Soc. China* 22 (2012) 983–990.
- [9] Q. Lu, J. Yu, J. Gao, Degradation of 2,4-dichlorophenol by using glow discharge electrolysis, *J. Hazard. Mater.* 136 (2006) 526–531.
- [10] P. Jiang, J. Zhou, A. Zhang, Y. Zhong, Electrochemical degradation of p-nitrophenol with different processes, *J. Environ. Sci.* 22 (2010) 500–506.
- [11] Z. Wu, D. Zhao, Ordered mesoporous materials as adsorbents, *Chem. Commun.* 47 (2011) 3332–3338.
- [12] M.R. Awual, T. Yaita, S.A. El-Safty, H. Shiwaku, S. Suzuki, Y. Okamoto, Copper(II) ions capturing from water using ligand modified a new type mesoporous adsorbent, *Chem. Eng. J.* 221 (2013) 322–330.
- [13] T. Yokoi, Y. Kubota, T. Tatsumi, Amino-functionalized mesoporous silica as base catalyst and adsorbent, *Appl. Catal. A* 421–422 (2012) 14–37.
- [14] J. Brown, R. Richer, L. Mercier, One-step synthesis of high capacity mesoporous Hg²⁺ adsorbents by non-ionic surfactant assembly, *Micropor. Mesopor. Mater.* 37 (2000) 41–48.
- [15] X.-W. Wu, H.-W. Ma, J. Yang, F.-J. Wang, Z.-H. Li, Adsorption of Pb(II) from aqueous solution by a poly-elemental mesoporous adsorbent, *Appl. Surf. Sci.* 258 (2012) 5516–5521.
- [16] A.S. Barreto, A. Aquino, S.C.S. Silva, M.E. de Mesquita, M.J. Calhorda, M.S. Saraiva, S. Navickiene, A novel application of mesoporous silica material for extraction of pesticides, *Mater. Lett.* 65 (2011) 1357–1359.
- [17] M.Z. Momčilović, M.S. Randelović, A.R. Zarubica, A.E. Onjia, M. Kokunešoski, B.Z. Matović, SBA-15 templated mesoporous carbons for 2,4-dichlorophenoxyacetic acid removal, *Chem. Eng. J.* 220 (2013) 276–283.
- [18] I. Muylaert, A. Verberckmoes, J. De Decker, P. Van der Voort, Ordered mesoporous phenolic resins: highly versatile and ultra stable support materials, *Adv. Colloid Interf. Sci.* 175 (2012) 39–51.
- [19] R. Ryoo, S.H. Joo, S. Jun, Synthesis of highly ordered carbon molecular sieves via template-mediated structural transformation, *J. Phys. Chem. B* 103 (1999) 7743–7746.
- [20] Q. Liu, A. Wang, X. Wang, T. Zhang, Ordered crystalline alumina molecular sieves synthesized via a nanocasting route, *Chem. Mater.* 18 (2006) 5153–5155.
- [21] S.H. Joo, S.J. Choi, I. Oh, J. Kwak, Z. Liu, O. Terasaki, R. Ryoo, Ordered nanoporous arrays of carbon supporting high dispersions of platinum nanoparticles, *Nature* 412 (2001) 169–172.
- [22] D. Zhao, Q. Huo, J. Feng, B. Chmelka, G. Stucky, Nonionic triblock and star diblock copolymer and oligomeric surfactant syntheses of highly ordered, hydrothermally stable, mesoporous silica structures, *J. Am. Chem. Soc.* 120 (1998) 6024–6036.
- [23] A. Thomas, Functional materials: from hard to soft porous frameworks, *Angew. Chem. Int. Ed.* 49 (2010) 8328–8344.
- [24] Y. Wan, Y. Shi, D. Zhao, Supramolecular aggregates as templates: ordered mesoporous polymers and carbons, *Chem. Mater.* 20 (2007) 932–945.
- [25] M. Bosetto, P. Arfaio, P. Fusi, Adsorption of the herbicides alachlor and metolachlor on two activated charcoals, *Sci. Total Environ.* 123–124 (1992) 101–108.
- [26] X.M. Wu, M. Li, Y.H. Long, R.X. Liu, Y.L. Yu, H. Fang, S.N. Li, Effects of adsorption on degradation and bioavailability of metolachlor in soil, *J. Soil Sci. Plant Nutr.* 11 (2011) 83–97.
- [27] L. Allievi, C. Gigliotti, C. Salardi, G. Valsecchi, T. Brusa, A. Ferrari, Influence of the herbicide bentazon on soil microbial community, *Microbiol. Res.* 151 (1996) 105–111.
- [28] A. Omri, A. Wali, M. Benzina, Adsorption of bentazon on activated carbon prepared from Lawsonia inermis wood: equilibrium, kinetic and thermodynamic studies, *Arab. J. Chem.* <http://dx.doi.org/10.1016/j.arabjc.2012.04.047>
- [29] D. Grosso, F. Cagnol, G.J.d.A.A. Soler-Illia, E.L. Crepaldi, H. Amenitsch, A. Brunet-Bruneau, A. Bourgeois, C. Sanchez, Fundamentals of mesostructuring through evaporation-induced self-assembly, *Adv. Funct. Mater.* 14 (2004) 309–322.
- [30] C.-K. Tsung, J. Fan, N. Zheng, Q. Shi, A.J. Forman, J. Wang, G.D. Stucky, A general route to diverse mesoporous metal oxide microspheres with highly crystalline frameworks, *Angew. Chem. Int. Ed.* 47 (2008) 8682–8686.
- [31] J. Jin, N. Nishiyama, Y. Egashira, K. Ueyama, Pore structure and pore size controls of ordered mesoporous carbons prepared from resorcinol/formaldehyde/triblock polymers, *Micropor. Mesopor. Mater.* 118 (2009) 218–223.
- [32] S. Lagergren, Zur theorie der sogenannten adsorption gel oster stoffe, *Kungliga Svenska Vetenskapsakademiens* 24 (1898) 1–39.
- [33] Y.S. Ho, G. McKay, Pseudo-second order model for sorption processes, *Process Biochem.* 34 (1999) 451–465.
- [34] J.C. Morris, W.J. Weber, Kinetics of adsorption of carbon from solutions, *J. Sanit. Eng. Div. Am. Soc. Civ. Eng.* 89 (1963) 31–63.
- [35] H.M.F. Freundlich, Ober Die Adsorption in Lösungen, *Zeitschrift Für Physikalische Chemie* 57 (1906) 385.
- [36] I. Langmuir, The adsorption of gases on plane surfaces of glass, mica and platinum, *J. Am. Chem. Soc.* 40 (1918) 1361–1403.

- [37] O. Çelebi, C. Üzümlü, T. Shahwan, H.N. Erten, A radiotracer study of the adsorption behavior of aqueous Ba^{2+} ions on nanoparticles of zero-valent iron, *J. Hazard. Mater.* 148 (2007) 761–767.
- [38] M.M. Dubinin, L.V. Radushkevich, *Zh. Fiz. Khim.* 55 (1947) 327.
- [39] U. Ciesla, F. Schüth, Ordered mesoporous materials, *Micropor. Mesopor. Mater.* 27 (1999) 131–149.
- [40] N. Farzin Nejad, E. Shams, M.K. Amini, J.C. Bennett, Synthesis of magnetic mesoporous carbon and its application for adsorption of dibenzothiophene, *Fuel Process. Technol.* 106 (2013) 376–384.
- [41] C.O. Ania, F. Béguin, Mechanism of adsorption and electrosorption of bentazone on activated carbon cloth in aqueous solutions, *Water Res.* 41 (2007) 3372–3380.
- [42] A. Boivin, R. Cherrier, M. Schiavon, A comparison of five pesticides adsorption and desorption processes in thirteen contrasting field soils, *Chemosphere* 61 (2005) 668–676.
- [43] T.L. Grey, G.R. Wehtje, R.H. Walker, Sorption and mobility of bentazone in coastal plain soils, *Weed Sci.* 44 (1996) 166–170.
- [44] M. Islam, R. Patel, Nitrate sorption by thermally activated Mg/Al chloride hydrotalcite-like compound, *J. Hazard. Mater.* 169 (2009) 524–531.
- [45] R. Otero, J.M. Fernández, M.A. González, I. Pavlovic, M.A. Ulibarri, Pesticides adsorption–desorption on Mg–Al mixed oxides. Kinetic modeling, competing factors and recyclability, *Chem. Eng. J.* 221 (2013) 214–221.
- [46] C.H. Giles, T.H. Macewan, S.N. Nakhwa, D. Smith, Studies in adsorption. 11. A system of classification of solution adsorption isotherms, and its use in diagnosis of adsorption mechanisms and in measurement of specific surface areas of solids, *J. Chem. Soc.* (1960) 3973–3993.
- [47] A.S. Özcan, Ö. Gök, A. Özcan, Adsorption of lead(II) ions onto 8-hydroxy quinoline-immobilized bentonite, *J. Hazard. Mater.* 161 (2009) 499–509.
- [48] M. Islam, R. Patel, Polyacrylamide thorium (IV) phosphate as an important lead selective fibrous ion exchanger: synthesis, characterization and removal study, *J. Hazard. Mater.* 156 (2008) 509–520.
- [49] S.K. Milonjic, A consideration of the correct calculation of thermodynamic parameters of adsorption, *J. Serb. Chem. Soc.* 72 (2007) 1363–1367.
- [50] Muhammad, M.A. Khan, T.S.Y. Choong, T.G. Chuah, R. Yunus, Y.H.T. Yap, Desorption of β -carotene from mesoporous carbon coated monolith: isotherm, kinetics and regeneration studies, *Chem. Eng. J.* 173 (2011) 474–479.
- [51] K. Misra, S.K. Kapoor, R.C. Bansal, Regeneration of granular activated carbon loaded with explosives, *J. Environ. Monit.* 4 (2002) 462–464.
- [52] P.S. Suchithra, L. Vazhayal, A. Peer Mohamed, S. Ananthakumar, Mesoporous organic–inorganic hybrid aerogels through ultrasonic assisted sol–gel intercalation of silica–PEG in bentonite for effective removal of dyes, volatile organic pollutants and petroleum products from aqueous solution, *Chem. Eng. J.* 200–202 (2012) 589–600.